Bet-hedging and epigenetic inheritance in bacterial cell development

Jan-Willem Veening*†, Eric J. Stewart‡§¶, Thomas W. Berngruber‖, François Taddei‡§, Oscar P. Kuipers*,**, and Leendert W. Hamoen†

*Molecular Genetics Group, Groningen Biomolecular Sciences and Biotechnology Institute, and ‖Theoretical Biology Group, Centre for Ecological and Evolutionary Studies, University of Groningen, 9751 NN, Haren, The Netherlands; ‡Institut National de la Santé et de la Recherche Médicale, U571, Université Paris, 75015 Paris, France; §Faculty of Medicine, Paris Descartes University, F-75015 Paris, France; and †Institute for Cell and Molecular Biosciences, Newcastle University, Newcastle upon Tyne NE2 4HH, United Kingdom

Upon nutritional limitation, the bacterium *Bacillus subtilis* has the capability to enter the irreversible process of sporulation. This developmental process is bistable, and only a subpopulation of cells actually differentiates into endospores. Why a cell decides to sporulate or not to do so is poorly understood. Here, through the use of time-lapse microscopy, we follow the growth, division, and differentiation of individual cells to identify elements of cell history and ancestry that could affect this decision process. These analyses show that during microcolony development, *B. subtilis* uses a bet-hedging strategy whereby some cells sporulate while others use alternative metabolites to continue growth, providing the latter subpopulation with a reproductive advantage. We demonstrate that *B. subtilis* is subject to aging. Nevertheless, the age of the cell plays no role in the decision of its fate. However, the physiological state of the cell's ancestor (more than two generations removed) does affect the outcome of cellular differentiation. We show that this epigenetic inheritance is based on positive feedback within the sporulation phosphorelay. The extended intergenerational ''memory'' caused by this autostimulatory network may be important for the development of multicellular structures such as fruiting bodies and biofilms.

aging | *Bacillus subtilis* | bistability | sporulation

Developmental switches that govern cell fate decisions are often based on interlinked feedback loops (1). Importantly, such feedback-based switches can generate bistability; i.e., the occurrence of two distinct subpopulations that exhibit different phenotypes within the isogenic population (2). Maturation in developing oocytes in *Xenopus* embryos is governed by a bistable switch, and the Hedgehog network, responsible for cellular differentiation in a diversity of eukaryotes, involves bistable switching as well (3, 4). These types of regulatory switches are also found in single-celled organisms such as yeasts and bacteria, where they lead to phenotypic variability within the isogenic population (2). Based on mathematical modeling and synthetic gene-regulatory networks, it was shown that stochasticity in gene expression (referred to as noise), when amplified by positive feedback, can be the generator of a bistable response (5). However, intrinsic physiological parameters, such as the cell cycle and cell age, are known contributors to phenotypic variability as well (6). Whether the outcome of a bistable cellular differentiation process is influenced by such physiological parameters or whether it is purely a stochastic phenomenon is unknown. It is also unclear how far in advance of the appearance of the phenotypic change such decisions are made. Here, we use *Bacillus subtilis*, a model organism for studying bacterial cell developmental processes, to address these questions.

When nutrient sources are dwindling, *B. subtilis* cells can sporulate by forming a highly resistant endospore at one cell pole, which is later released by lysis of the mother cell (7). It was shown that the complex positive-feedback architecture of the sporulation signal transduction cascade is pivotal for this developmental program to behave as a (unidirectional) bistable switch (8, 9). This bistability is exemplified by the presence of two distinct subpopulations within the isogenic culture: sporulating and nonsporulating cells. It is generally assumed that the decision to sporulate is stochastic in nature, although direct experimental evidence for this assumption has never been provided (10, 11). Moreover, there are several potential nonstochastic phenomena that may play a role in the decision to sporulate, such as the cell history, cell cycle timing, and cell age (2, 6). To investigate these potential influences, we designed an experimental procedure using quantitative time-lapse microscopy, which allows us to follow the outgrowth of a single *B. subtilis* cell into a sporulating microcolony.

Results

Sporulation in a Microcolony. Microscopic observation of a growing microcolony has been used to examine cell aging in *Escherichia coli* (12). Here, we adopted this technique to study the origins of the sporulation decision in *B. subtilis*. The medium and growth conditions were adjusted so that single cells grew into sporulating microcolonies of approximately a few hundred cells [for more details, see supporting information (SI) *Materials and Methods*]. An example of a sporulating microcolony is shown in Fig. 1A. Growth of *B. subtilis* within such microcolonies follows a classical pattern with exponential growth followed by a period of reduced growth rate, termed the diauxic shift, after which growth ceases, and the first endospores become visible (Fig. 1B). This secondary growth phase is probably caused by the utilization of overflow metabolites, such as acetoin, after the disappearance of glucose (13). After the cessation of the secondary growth phase, there is a period of ≈10 h during which there is no cell growth. However, there is considerable cell lysis during this period, and more than half of all cells die [Fig. 1A and B (69% ± 10% lysis measured in five colonies)]. After this period of apparent dormancy, part of the remaining cells resume growth, probably by using the nutrients released from the lysed cells, and a new round of growth and sporulation takes place (Fig. 1B, SI Fig. 6, and SI Movies 1–3). Spores formed during the growth of the microcolony were never observed to germinate during this new growth period.

To visualize the physiological state of individual cells conveniently in a single graph, we calculated the growth rate of each cell as an exponential fit to the length measurements of the cell at all

© 2008 by The National Academy of Sciences of the USA

MICROBIOLOGY
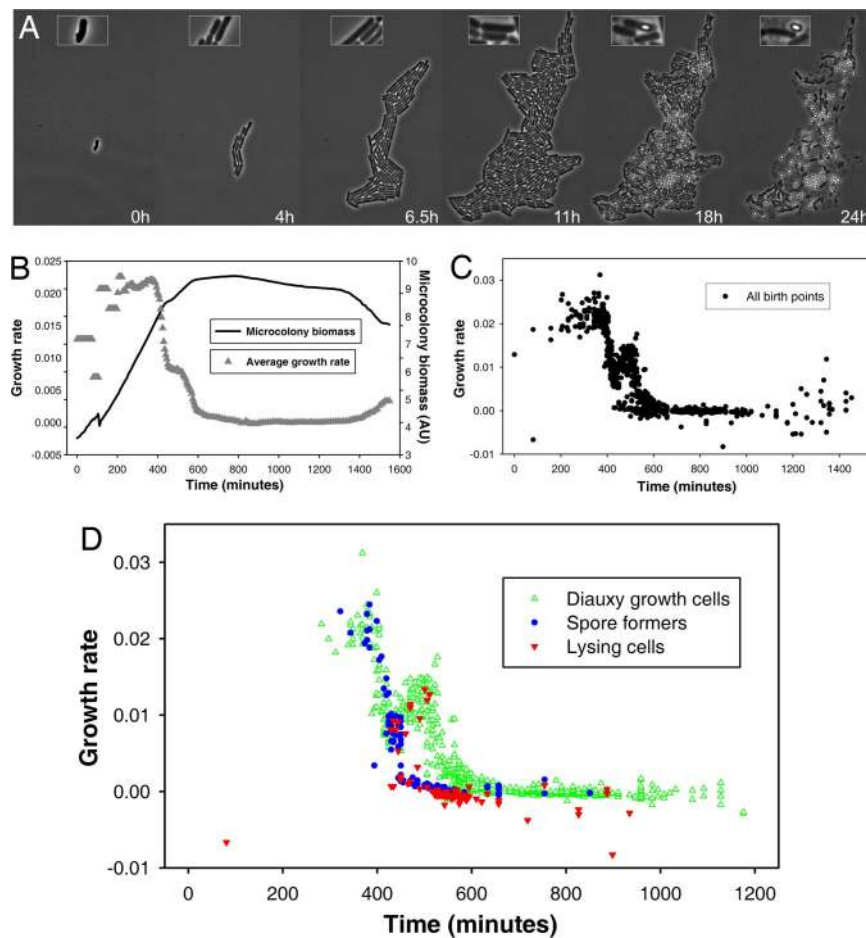
Fig. 1. Typical *B. subtilis* microcolony development. (*A*) Still frames (phase contrast) of the outgrowth of a single cell into a sporulating microcolony. (*Insets*) Magnifications. (*B*) Log of microcolony biomass (black line) and average growth rates (gray triangles) are plotted in time. The growth rate is calculated as an exponential fit to cell length in time (arbitrary units, AU), measured from the birth point of the cell until the next cell division event or cell fate decision (see *SI Materials and Methods*). Biomass was calculated as a function of cell length (AU). (*C*) Each circle represents the point of birth in time of an individual cell. The average growth rate of this cell during its life is represented on the *y* axis (AU). (*D*) Cell fates plotted onto the birth points of *C*. Every birth point shown indicates the birth of a cell for which it is certain that either this cell or all of its descendents will follow a specific fate. Blue circles show the growth rates of individual cells committed to spore formation; green triangles show diauxic growth fate cells; and red triangles indicate lysing cells.

time points between its birth and subsequent division. Because cells only grow in length and not in width, the exponential length increase is a good measurement of growth rate. It yielded a single value for the growth rate of each cell, which was then plotted at the time of birth of that cell (Fig. 1*C*). Surprisingly, this graph shows that during the diauxic shift, many cells do not use the overflow metabolites to resume cellular growth.

Three morphologically identifiable cell fates that arise after the initial exponential growth can be distinguished: spore-forming cells, lysing cells, and those that survive as vegetative cells. Using custom software (see *SI Materials and Methods*), we traced the history and lineage of every individual cell, enabling us to determine the point in the lineage at which the fate of a newborn cell is fixed. This point was visualized by plotting the different fates on a birth time vs. growth rate graph, similar to Fig. 1*C*. Every birth point shown indicates the birth of a cell for which it is certain that either this cell or all of its descendents will follow a specific viable fate. For clarity, we focused on the first 20 h of the microcolony existence, before the later second round of growth and spore formation. The resulting graph (Fig. 1*D*) reveals an intriguing insight into the differentiation of a *B. subtilis* cell population. The fate of many cells is already fixed at the end of the exponential growth phase, but most surprising is the separation in cell fate decisions that occurs during the diauxic shift. Cells that eventually sporulate do not grow during this period, whereas vegetative cells, which will not sporulate during this growth phase, do continue to grow (diauxic growth cells). Lineages that will exclusively have lysis as a cell fate only appear later and are distributed between the two viable cell fate paths [i.e., sporulation and diauxic growth (SI Fig.7)]. Clearly, the belief that the only cells that contribute to the perpetuation of a *B. subtilis* population that has exhausted the primary nutrients are those that sporulate needs

revision. It appears that the alternative to sporulation is to use secondary metabolites to continue growth as long as possible. In fact, under these conditions, this alternative path results in a numerical advantage and thus contributes more to the future of the population (in terms of potentially viable cells and spores) than the initial, early sporulation path (SI Table 1).

Lysis Does Not Depend on the Sporulation Killing Factors. Sporulating cells express the *skf* and *sdp* operons whose gene products are responsible for the export of killing factors that induce lysis (14). Vegetative cells are sensitive to these killing factors, and it has been suggested that the sporulating cells use the nutrients released by their killed siblings and thereby delay or prevent full commitment to spore formation. This phenotypic behavior occurs predominantly under high-cell-density conditions as in dense colonies on agar plates. However, under the growth conditions in our work, lysis within microcolonies did not depend on the presence of these killing factors (SI Movie 4).

***B. subtilis* Undergoes Aging, but This Process Does Not Affect Cell Fate.** The question remains as to what determines the decision to sporulate or to follow the diauxic growth path. We considered the possibility that the aging of the cell plays a role. For instance, in yeast, aging is a driving force in generating phenotypic variation, resulting in subpopulations of cells with different resistances to oxidative stress (15). Rod-shaped bacteria, such as *B. subtilis* and *E. coli*, divide by binary fission whereby cell division takes place at midcell (16). The newly formed division septum will become a new cell pole after cytokinesis has completed. As a result of this symmetrical cell division, two morphologically identical "progeny" cells are formed; however, these two cells differ with respect to the
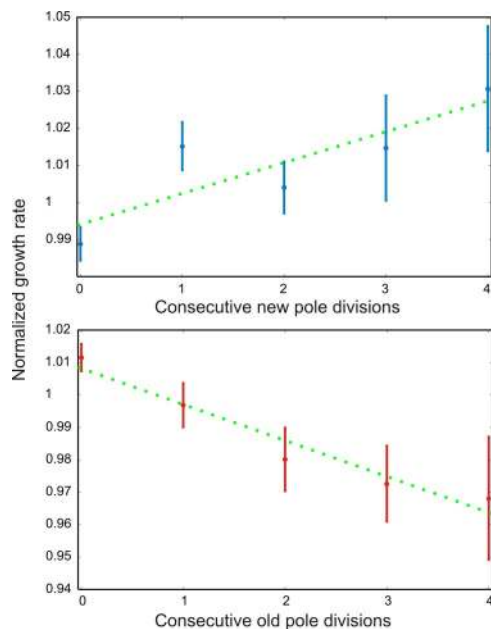
Fig. 2. Aging in *B. subtilis*. Effects of consecutive divisions as a new pole cells (blue circles, showing rejuvenation) or old pole cells (red circles, showing aging). Error bars represent the SEM. Trend lines are shown in green (the actual progressions may not be linear). See also SI Fig. 8 and ref. 12.

age of their poles. Recently, it was shown that this difference in pole age is physiologically significant for *E. coli*; the cell inheriting the old pole suffers from aging and exhibits a decreased growth rate, less offspring production, and an increased probability of death (12). To determine whether cell aging could play a role in *B. subtilis* cell differentiation, it was necessary first to establish the presence of aging in this organism. The lineages from 10 separate microcolonies (during the primary, glucose-based phase of growth) were determined based on cell pole age (inspecting a total of 1,080 cells). As shown in Fig. 2 and SI Fig. 8, *B. subtilis* cells show a significant aging effect during vegetative growth. Despite the presence of aging, statistical tests for age-related bias in the subpopulation of cells that committed to sporulation show that, on average, sporulating cells are not significantly older or younger than non-spore formers (expected average pole age of 106 sporulating cells from two

independent films, 1.00; actual age, 1.08; $P = 0.60$) (see SI Materials and Methods). Similarly, cells that ultimately lysed were tested for cell age bias, and also in this case there was no relation with cell pole age (expected average pole age of 729 lysing cells from two independent films, 1.00; actual age, 1.02; $P = 0.67$). Finally, the pole age of cells that initially commit to diauxic growth were also analyzed, with no significant bias in pole age found (expected average pole age of 284 diauxic growth cells from two independent films, 1.00; actual age, 1.03; $P = 0.71$). Taken together, these data demonstrate that cell age is not a factor that determines the fate of *B. subtilis* cells.

A replication checkpoint system in *B. subtilis* ensures that sporulation does not initiate when cells are not in their correct cell cycle (17). Therefore, we looked for cell cycle-related physiological parameters that might distinguish spore formers from non-spore formers, and we closely examined and compared birth times, growth rates, and cell length of cells demonstrating these two fates (SI Fig. 9). These analyses did not reveal any apparent differences in any of the measured parameters between the two cell types. Because we could not identify any age- or cell cycle-related bias toward spore formation, this analysis strengthens the supposition that the initial decision to sporulate is stochastic in its origin.

Previous work has shown that in liquid media, the endospore is preferably formed at the old pole of the cell (18). An analysis of the position of the endospore of spore formers in microcolonies showed that they were formed at the old pole in 79 of the 162 recorded cases (49%), indicating that there is no significant preference for spores to form at the old or new pole within microcolonies on solid media.

Cell Lineage History Influences Cell Fate. As shown in Fig. 1*D*, cells that will sporulate do not grow during the diauxic shift, which suggests that the timing of activation of the main sporulation transcription regulator, Spo0A, differs substantially between cells. Spo0A is directly responsible for the initiation of sporulation; but to become active, Spo0A needs to be phosphorylated, which is achieved through a complex phosphorelay involving multiple phosphotransferases and phosphatases on which environmental signals act (19). Using standard light microscopy, only the late stages of sporulation can be followed. To visualize the induction of the sporulation cascade at an earlier point during development, we fused the gene encoding green fluorescent protein (*gfp*) to the Spo0A~P-inducible *spoIIA* promoter (*spoIIA-gfp*). When microcolonies reached the stationary growth phase, part of the population begins to express GFP (Fig. 3*A* and SI Movies 1 and 2). These

<div style="text-align: right;">MICROBIOLOGY</div>
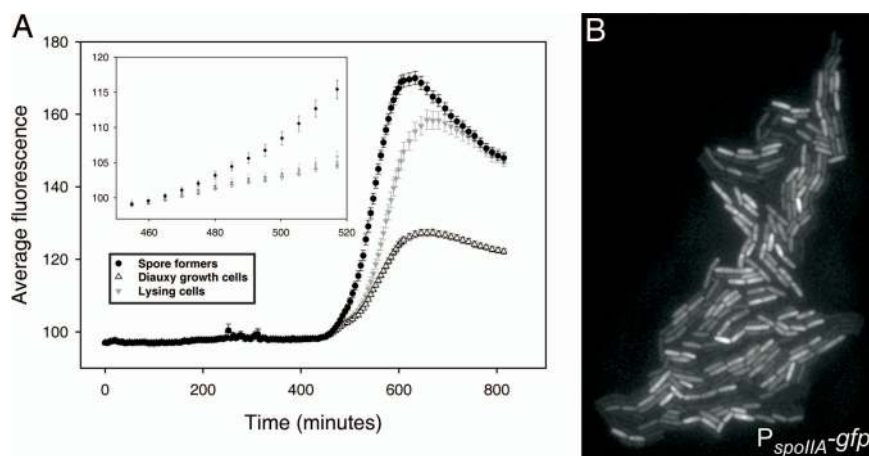
Fig. 3. Lineage-related expression of cell fates. (*A*) Average *gfp* expression from the *spoIIA* promoter of subpopulations of cells with different cell fates. For clarity, the fluorescence of only the first 13 h of the microcolony existence, before the later second round of growth and spore formation, is depicted. The SEM is indicated by error bars. (*Inset*) Magnification of the period between 460 and 520 min. (*B*) Fluorescence image of a *B. subtilis* microcolony after ≈12 h of growth when the microcolony consisted of 408 cells.

Fig. 4. Inheritance in the decision to sporulate. (*A*) Parsimony mapping of the fluorescence character (GFP) onto the true lineage tree of 356 cells. Red tips, cells with fluorescence value above 40 fluorescence units. Black tips, cells below this threshold. (*B*) Parsimony mapping of fate information onto the true lineage tree of 531 cells. Every end point in the tree represents one offspring cell; red tips, spore-forming cells. Detailed parsimony character mappings are shown in SI Fig. 12.

cells are also the first to differentiate into spores (SI Fig. 10). Eventually, all cells within the microcolony will express GFP to some level (Fig. 3*A*). Lysing cells also show a range of induction levels of GFP, confirming our observation from the growth rate graph in Fig. 1 that lysing cells arise in both the sporulation and diauxic-growth pathways (SI Fig. 11). Again, no apparent difference in any of the measurable physiological parameters (cell length, birth point, etc.) could be distinguished between cells that activated *spoIIA-gfp* at an early stage and cells that did not.

A striking observation of the time-lapse films was that fluorescent cells appear to group in families, seen as long lineages of cells oriented end-to-end. These strings of fluorescent cells are often immediately adjacent to families of cells that express no or low levels of GFP (Fig. 3*B*). When we examined a strain that carries a GFP–reporter that is specifically repressed by Spo0A~P (P$_{abrB}$-*gfp*), families of fluorescent and nonfluorescent cells were also observed (SI Movie 5). Sporulating cells also show spatial clustering, albeit weak, as demonstrated by a randomized nearest-neighbor analysis (see *SI Materials and Methods*).

Because lineages of related cells form linear groupings within the microcolony, we examined whether this spatial correlation might arise from an underlying lineage correlation. To assess whether *spoIIA*-inducing and sporulating cells are closely related or randomly distributed within the genealogy, we used parsimony reconstruction of ancestral cell states. Parsimony reconstruction estimates the history of cell fates by minimizing the total number of changes in the fate decisions that have occurred over the history of the tree (for a more detailed description, see ref. 21). In this way, the first appearance of a mother cell that creates offspring of mostly *spoIIA-gfp*-expressing and sporulating cells can be estimated. As shown in Fig. 4*A*, expression of GFP from the *spoIIA* promoter is highly lineage-dependent and can often be traced back for more than four cell divisions within the microcolony lineage tree (for higher resolution, see SI Fig. 12).

To check that the observed lineage dependence in fluorescence was not generated merely by dilution of already-expressed GFP among the offspring, we performed an extensive analysis on the fluorescence profiles throughout the lineage from cells that cluster together (see SI Fig. 13). Indeed, *spoIIA-gfp* activation at the time point used for the parsimony reconstruction (669 min) occurs mainly concurrently among closely related cells after the lineage has been established, indicating that the decision to sporulate occurs upstream of the *spoIIA* promoter and GFP induction (SI Fig. 13).

We conclude that the signal to activate Spo0A propagated from a common ancestor, and because these cell fates are not caused by genetic mutations, the cell state inherited from the ancestor must be epigenetic. Analysis of parsimony reconstruction using actual

spore formation as a phenotype also showed clustering within the lineage tree and can often be traced back more than two cell divisions within the microcolony lineage (Fig. 4*B* and SI Figs. 12 and 14). As a control, we tested whether these clustered trees could be generated by a random process alone. To do so, we assessed with a statistical test for phylogenetic signal (20) whether closely related cells are more likely to express the same phenotype. The mean squared error (MSE) of independent "phylogenetic contrasts" for the observed and randomized trees were calculated as described in ref. 20 (SI Fig. 15) (for spore formation: observed MSE = 0.102, mean MSE of permuted data = 0.179, $P < 0.001$; for GFP expression: observed MSE = 337, mean MSE of permuted data = 847, $P < 0.001$). This analysis demonstrated that the phylogenetic clustering of GFP expression, or spores, is not a random process and indicates that families of cells are more likely to share the same phenotype in a differentiating *B. subtilis* colony.

Epigenetic Inheritance Depends on the Phosphorelay. For epigenetic inheritance to occur, the sporulation signal must be preserved over multiple generations. Therefore, it is likely that the signal is reinforced and maintained during growth and division. The auto-stimulatory architecture of the Spo0A regulation cascade comprises several positive-feedback loops that could be responsible for this phenomenon (2). For example, Spo0A~P binds to its own promoter to stimulate transcription, and expression of *kinA*, encoding the primary kinase of the phosphorelay, is indirectly activated by Spo0A~P (22). We first examined whether the positive feedback of *spo0A* transcription is responsible for the families of *spoIIA*-GFP-expressing cells. To do so, we constructed a strain where the native promoter of *spo0A* was replaced by an IPTG-inducible promoter (P$_{spac}$) (Fig. 5*A*). Previous work had shown that wild-type levels of Spo0A are achieved with this promoter when a concentration of ≈40 μM IPTG is used (8). Time-lapse analysis of this strain growing on an agarose patch containing medium with 40 μM IPTG clearly shows two subpopulations in fluorescence distribution and the presence of subfamilies (Fig. 5*C*, SI Fig. 16, and SI Movie 6). Even when Spo0A is overproduced by growing cells in the presence of 100 μM IPTG, *spoIIA-gfp* expression is bimodal, but now more cells activate *spoIIA-gfp* and sporulate (SI Fig. 16 and SI Movie 7). These experiments show that autostimulatory transcription of *spo0A* is not essential for bistable expression (and sporulation) or for epigenetic inheritance of the sporulation signal. To examine the importance of the phosphorelay in this process, the constitutively active mutant variant of Spo0A (Sad67) was tested. This mutant protein does not require phosphorylation by the phosphorelay to activate sporulation gene expression (23, 24). Thus, a strain harboring the *sad67* gene under the control of the *spac* promoter lacks any putative positive-feedback loop acting on *spo0A* transcription or Spo0A phosphorylation (Fig. 5*B*). As shown in Fig. 5*D*, SI Fig. 16, and SI Movie 8, in the presence of 40 μM IPTG, all cells gradually and synchronously express *spoIIA-gfp*, and subfamilies are no longer established. These data suggest that the phosphorelay is important for both bistable induction of *spo0A* and the propagation of the Spo0A activation signal. In fact, by removing a major phosphatase (RapA) of the phosphorelay (25), the number and size of subfamilies that express *spoIIA-gfp* increase (SI Fig. 17 and SI Movie 9). Artificial induction of another phosphorelay phosphatase (Rap60) (26) gave the opposite effect and resulted in strikingly smaller subfamilies (SI Fig. 17 and SI Movie 9).

Discussion

By following a growing *B. subtilis* microcolony in detail, we came across some unexpected findings. The total growth rate of a microcolony follows a classic curve with an exponential phase followed by a diauxic phase. Surprisingly, it appeared that the diauxic growth phase is exclusively used by nonsporulating cells (Fig. 1). Because spore formation is a long and energy-intensive process, it is plausible that sporulating cells use the overflow

Fig. 5. Phosphorelay is required to generate subfamilies. (*A* and *B*) Schematic diagram of the regulatory cascade present in strains IIA/Δ0A/spo0A and IIA/spo0A/sad67, respectively. (*C* and *D*) Time-lapse microscopy of strains IIA/Δ0A/spo0A (P$_{spac}$-*spo0A*) and IIA/spo0A/sad67 (P$_{spac}$-*sad67*). Membranes are stained by FM5–95 (red), and GFP is depicted in green.

metabolites to complete this cell fate. The induction of overflow metabolism can be monitored by following the expression of the acetoin catabolic pathway (*acoA-L*), which is exclusively activated when the growth medium is exhausted for glucose (13). Indeed, we found that all cells in a microcolony express this operon at the end of the logarithmic growth phase (SI Fig. 18 and SI Movie 10). That the sporulating cells do not continue to grow is likely caused by the elevated concentrations of Spo0A~P in these cells because high levels of Spo0A~P inhibit symmetrical (vegetative) cell division (27).

Cells that do not sporulate when nutrients become limiting are not lost. By following the diauxic growth fate, their numbers increase, and they may sporulate later by using nutrients released by cells that have lysed. Moreover, these "diauxic growers" are ready to begin rapid growth in case there is a new influx of nutrients. In contrast, the "sporulators" are committed to a long-term process of spore formation and germination (7). Thus, each of these pathways is a form of cell specialization. One benefit of the simultaneous presence of both pathways is the optimal use of resources in the long run. As mother cells lyse to release the endospores, they also release cellular components that could be used as a source of nutrients. In other words, heterogeneity in the timing of spore formation allows utilization of these resources that would otherwise be lost. Maybe even more important is that these two fates have different reproductive potential under different environments. Because the future is not predictable, the clonal population profits by being prepared for a variety of future environments, a form of bet-hedging (28, 29).

The *B. subtilis* laboratory strain commonly used, and also used in this work, is a poor sporulator compared with some natural isolates (10). Because this strain has been propagated in the laboratory for many decades, it might be that it is evolutionary optimized to colonize rapidly from vegetative (diauxic) growing cells. Although this condition is potentially a response to human-imposed conditions, natural environments with similar fluctuating nutrient levels may result in the evolution of similar distributions of the bistable states.

A third cell fate in a maturing *B. subtilis* colony is cell lysis, and it may represent a failure to complete the preferred differentiation pathway. Under our experimental setup, the sporulation killing factors are not responsible for lysis, indicating a role for other intrinsic or extrinsic causes.

Cellular aging is a universal phenomenon that also affects bacteria, as has been shown for the proteobacteria *E. coli* and *Caulobacter crescentus* (12, 30). Here, we demonstrate aging in a bacterium outside this phylogenetic group (Fig. 2). Older *B. subtilis* cells show a clear reduction in growth rate, but cell pole age did not appear to play a determining role in the choice to sporulate, follow diauxic growth, or lyse. We also looked at other differences that might bias cells to a specific fate, such as birth time, cell length, or growth rate (markers for cell cycle timing and physiological state). Again, no relation with the separate fates could be identified (SI Fig. 9). Previous work has shown that sporulation can only occur when the chromosome is in a particular stage of replication (31, 32). It will be interesting to see the importance of the replication state on the final bifurcation of the differentiation pathways.

When we examined GFP reporter strains that are specific for Spo0A activation (P$_{spoIIA}$-*gfp* and P$_{abrB}$-*gfp*), we noticed that GFP-expressing cells were often clustered (Fig. 3). Such groups of cells appeared to be phylogenetically related, suggesting that the signal to activate Spo0A is epigenetically inherited (Fig. 4 and SI Fig. 12). A general mechanism by which this inheritance can occur is through an intracellular positive-feedback loop (33). Maturation of *Xenopus* oocytes and the white-opaque phenotype in *Candida albicans*, for example, are governed by such a bistable positive-feedback memory module (34, 35); and by using artificial bistable gene regulatory circuits, epigenetic inheritance of semistable states has recently been described in *Saccharomyces cerevisiae* (36, 37). In the case of *B. subtilis* sporulation, the phosphorelay provides an excellent candidate for such a positive-feedback loop, and by testing several mutants we have shown that both sporulation bistability and subfamily formation depend on this signal transduction complex (Fig. 5 and SI Fig. 17). This finding indicates that the sporulation signal is "memorized" by the positive-feedback architecture of the Spo0A phosphorylation circuitry, which includes autophosphorylating kinases (e.g., KinA and KinB) that are directly and/or indirectly transcriptionally activated by Spo0A~P. The autostimulatory architecture of the phosphorelay seems to be responsible for

MICROBIOLOGY

both bistable differentiation and epigenetic inheritance. However, the mere presence of positive-feedback regulation does not automatically result in a memory response. For instance, for the development of genetic competence, another bistable differentiation process in *B. subtilis* that depends on positive feedback, it was found that cells were not significantly more likely to become competent if their sibling became competent (38).

The importance of epigenetic inheritance of cell fates on the population level may be based on the effect it has on neighboring cells. In bacterial colonies, which are sessile communities of cells, epigenetic inheritance affects those cells that are spatially grouped, in contrast to cells within planktonic cultures. The formation of biofilms requires systematic cell differentiation, and in *B. subtilis*, multicellular structure formation and sporulation are coordinated and intertwined by the action of Spo0A (11, 39, 40). We propose that epigenetic inheritance plays an important role in the formation of socially organized structures such as biofilms and fruiting bodies.

Materials and Methods

Strains. The construction of *B. subtilis* strains abrB-gfp, IIA-gfp, IIA-gfp/ΔrapA, IIA-gfp/Xrap, and IIA/spo0A/sad67 has been published (9, 40). The construction of strains acoA-gfp, IIA/skf/sdp, and IIA/Δ0A/spo0A is described in *SI Materials and Methods*.

Time-Lapse Microscopy. Cells were inoculated onto a thin semisolid agarose matrix attached to a microscope slide. Images were obtained by using time-lapse microscopy. For a detailed description of the growth and microscopy conditions, see *SI Materials and Methods*.

Data Analysis. Custom analysis software (12) was supplemented with software routines to identify, segment, track, link, and establish cell fate of *B. subtilis* cells. To correct tracking errors and include scoring for spore formation and cell lysis, frames were manually measured, generating datasets that include the complete history and fate of individual *B. subtilis* cells growing in these microcolonies.

These datasets include information on the number of division cycles, its length, width, fluorescence intensity, lineage information, and fate.

Phylogenetic Analyses. The parsimony reconstruction of ancestral states was carried out with *Mesquite* version 2.0 (http://mesquiteproject.org). Every node within the tree represents a cell division event. For Fig. 4*B*, lineage and cell fate data (spore formers vs. non-spore formers) after 25 h of growth were used. These data contained information from 531 cells (including those that sporulated at a later stage). To generate a parsimony map of fluorescence distribution within the lineage (Fig. 4*A*), fluorescence information of 356 cells after 669 min (≈11h) of growth was made binary (''on'' or ''off'') on the basis of the cutoff value of 40 arbitrary fluorescence units above background (see SI Fig. 19). When the fluorescence data are randomized and the parsimony states are reconstructed, significantly smaller families are observed (SI Fig. 12). To test whether closely related cells are more likely to show the same cell state (fluorescence) or fate (spore formation or not), we used a test for phylogenetic signal (20). The phylogenetic signal test was done on data for cell fate data (spore formers vs. non-spore formers) after 25 h of growth. Although we only show the results of one microcolony, this analysis was performed on the lineage and fate information of three independent microcolonies all showing significant ''phylogenetic signal.'' The phylogenetic signal test for fluorescence was done on data after 669 min of growth (note that we used continuous fluorescence data for the test, unlike the data used to generate Fig. 4*A*). The calculations were carried out as described in ref. 20 with the use of the original *Matlab* code kindly provided by Ted Garland.

1. Brandman O, Ferrell JE, Jr, Li R, Meyer T (2005) Interlinked fast and slow positive-feedback loops drive reliable cell decisions. *Science* 310:496–498.
2. Smits WK, Kuipers OP, Veening JW (2006) Phenotypic variation in bacteria: The role of feedback regulation. *Nat Rev Microbiol* 4:259–271.
3. Bagowski CP, Besser J, Frey CR, Ferrell JE, Jr (2003) The JNK cascade as a biochemical switch in mammalian cells: Ultrasensitive and all-or-none responses. *Curr Biol* 13:315–320.
4. Lai K, Robertson MJ, Schaffer DV (2004) The sonic hedgehog signaling system as a bistable genetic switch. *Biophys J* 86:2748–2757.
5. Kærn M, Elston TC, Blake WJ, Collins JJ (2005) Stochasticity in gene expression: From theories to phenotypes. *Nat Rev Genet* 6:451–464.
6. Avery SV (2006) Microbial cell individuality and the underlying sources of heterogeneity. *Nat Rev Microbiol* 4:577–587.
7. Piggot PJ, Losick R (2002) *Bacillus subtilis and Its Closest Relatives: From Genes to Cells*, eds Sonenshein AL, Losick R, Hoch JA (Am Soc Microbiol, Washington, DC), pp 483–517.
8. Fujita M, Gonzalez-Pastor JE, Losick R (2005) High- and low-threshold genes in the Spo0A regulon of *Bacillus subtilis. J Bacteriol* 187:1357–1368.
9. Veening JW, Hamoen LW, Kuipers OP (2005) Phosphatases modulate the bistable sporulation gene expression pattern in *Bacillus subtilis. Mol Microbiol* 56:1481–1494.
10. Maughan H, Nicholson WL (2004) Stochastic processes influence stationary-phase decisions in *Bacillus subtilis. J Bacteriol* 186:2212–2214.
11. Veening JW, Smits WK, Hamoen LW, Kuipers OP (2006) Single cell analysis of gene expression patterns of competence development and initiation of sporulation in *Bacillus subtilis* grown on chemically defined media. *J Appl Microbiol* 101:531–541.
12. Stewart EJ, Madden R, Paul G, Taddei F (2005) Aging and death in an organism that reproduces by morphologically symmetric division. *PLoS Biol* 3:e45.
13. Silbersack J, et al. (2006) An acetoin-regulated expression system of *Bacillus subtilis. Appl Microbiol Biotechnol* 73:895–903.
14. Gonzalez-Pastor JE, Hobbs EC, Losick R (2003) Cannibalism by sporulating bacteria. *Science* 301:510–513.
15. Aguilaniu H, Gustafsson L, Rigoulet M, Nystrom T (2003) Asymmetric inheritance of oxidatively damaged proteins during cytokinesis. *Science* 299:1751–1753.
16. Shapiro L, McAdams HH, Losick R (2002) Generating and exploiting polarity in bacteria. *Science* 298:1942–1946.
17. Burkholder WF, Kurtser I, Grossman AD (2001) Replication initiation proteins regulate a developmental checkpoint in *Bacillus subtilis. Cell* 104:269–279.
18. Dunn G, Mandelstam J (1977) Cell polarity in *Bacillus subtilis*: Effect of growth conditions on spore positions in sister cells. *J Gen Microbiol* 103:201–205.
19. Burbulys D, Trach KA, Hoch JA (1991) Initiation of sporulation in *B. subtilis* is controlled by a multicomponent phosphorelay. *Cell* 64:545–552.
20. Felsenstein J (2004) *Inferring Phylogenies* (Sinauer, Sunderland, MA).
21. Blomberg SP, Garland T, Jr, Ives AR (2003) Testing for phylogenetic signal in comparative data: Behavioral traits are more labile. *Evolution* 57:717–745.
22. Predich M, Nair G, Smith I (1992) *Bacillus subtilis* early sporulation genes kinA, spo0F, and spo0A are transcribed by the RNA polymerase containing sigma H. *J Bacteriol* 174:2771–2778.
23. Ireton K, Rudner DZ, Siranosian KJ, Grossman AD (1993) Integration of multiple developmental signals in *Bacillus subtilis* through the Spo0A transcription factor. *Genes Dev* 7:283–294.
24. Fujita M, Losick R (2005) Evidence that entry into sporulation in *Bacillus subtilis* is governed by a gradual increase in the level and activity of the master regulator Spo0A. *Genes Dev* 19:2236–2244.
25. Perego M, Hoch JA (2002) in *Bacillus subtilis and Its Closest Relatives: From Genes to Cells*, eds Sonenshein AL, Hoch JA, Losick R (Am Soc Microbiol, Washington, DC), pp 473–481.
26. Koetje EJ, Hajdo-Milasinovic A, Kiewiet R, Bron S, Tjalsma H (2003) A plasmid-borne Rap-Phr system of *Bacillus subtilis* can mediate cell density-controlled production of extracellular proteases. *Microbiology* 149:19–28.
27. Ben-Yehuda S, Losick R (2002) Asymmetric cell division in *B. subtilis* involves a spiral-like intermediate of the cytokinetic protein FtsZ. *Cell* 109:257–266.
28. Thattai M, van Oudenaarden A (2004) Stochastic gene expression in fluctuating environments. *Genetics* 167:523–530.
29. Kussell E, Leibler S (2005) Phenotypic diversity, population growth, and information in fluctuating environments. *Science* 309:2075–2078.
30. Ackermann M, Stearns SC, Jenal U (2003) Senescence in a bacterium with asymmetric division. *Science* 300:1920.
31. Dawes IW, Kay D, Mandelstam J (1971) Determining effect of growth medium on the shape and position of daughter chromosomes and on sporulation in *Bacillus subtilis. Nature* 230:567–569.
32. Hauser PM, Errington J (1995) Characterization of cell cycle events during the onset of sporulation in *Bacillus subtilis. J Bacteriol* 177:3923–3931.
33. Casadesus J, D'Ari R (2002) Memory in bacteria and phage. *Bioessays* 24:512–518.
34. Xiong W, Ferrell JE, Jr (2003) A positive-feedback-based bistable ''memory module'' that governs a cell fate decision. *Nature* 426:460–465.
35. Zordan RE, Miller MG, Galgoczy DJ, Tuch BB, Johnson AD (2007) Interlocking transcriptional feedback loops control white-opaque switching in *Candida albicans. PLoS Biol* 5:e256.
36. Kaufmann BB, Yang Q, Mettetal JT, van Oudenaarden (2007) A heritable stochastic switching revealed by single-cell genealogy. *PLoS Biol* 5:e239.
37. Ajo-Franklin CM, et al. (2007) Rational design of memory in eukaryotic cells. *Genes Dev* 21:2271–2276.
38. Suel GM, Garcia-Ojalvo J, Liberman LM, Elowitz MB (2006) An excitable gene regulatory circuit induces transient cellular differentiation. *Nature* 440:545–550.
39. Branda SS, Gonzalez-Pastor JE, Ben-Yehuda S, Losick R, Kolter R (2001) Fruiting body formation by *Bacillus subtilis. Proc Natl Acad Sci USA* 98:11621–11626.
40. Veening JW, Kuipers OP, Brul S, Hellingwerf KJ, Kort R (2006) Effects of phosphorelay perturbations on architecture, sporulation, and spore resistance in biofilms of *Bacillus subtilis. J Bacteriol* 188:3099–3109.